



The University of
Nottingham

UNITED KINGDOM · CHINA · MALAYSIA

Stavroulakis, P.I. and Leach, Richard K. (2016) Review of post-process optical form metrology for industrial-grade metal additive manufactured parts. *Review of Scientific Instruments*, 87 (4). 041101/1-041101/15. ISSN 1089-7623

Access from the University of Nottingham repository:

<http://eprints.nottingham.ac.uk/32748/1/AM%20texture%20review.pdf>

Copyright and reuse:

The Nottingham ePrints service makes this work by researchers of the University of Nottingham available open access under the following conditions.

This article is made available under the University of Nottingham End User licence and may be reused according to the conditions of the licence. For more details see: http://eprints.nottingham.ac.uk/end_user_agreement.pdf

A note on versions:

The version presented here may differ from the published version or from the version of record. If you wish to cite this item you are advised to consult the publisher's version. Please see the repository url above for details on accessing the published version and note that access may require a subscription.

For more information, please contact eprints@nottingham.ac.uk

Invited Review Article: Review of post-process optical form metrology for industrial-grade metal additive manufactured parts

P. I. Stavroulakis and R. K. Leach

Citation: [Review of Scientific Instruments](#) **87**, 041101 (2016); doi: 10.1063/1.4944983

View online: <http://dx.doi.org/10.1063/1.4944983>

View Table of Contents: <http://scitation.aip.org/content/aip/journal/rsi/87/4?ver=pdfcov>

Published by the [AIP Publishing](#)

Articles you may be interested in

[Hardware-in-the-loop control of additive manufacturing processes using temperature feedback](#)

J. Laser Appl. **28**, 022302 (2016); 10.2351/1.4943911

[Laser powder bed fusion additive manufacturing of metals; physics, computational, and materials challenges](#)

Appl. Phys. Rev. **2**, 041304 (2015); 10.1063/1.4937809

[Compliance and control characteristics of an additive manufactured-flexure stage](#)

Rev. Sci. Instrum. **86**, 045107 (2015); 10.1063/1.4918982

[High-temperature oxidation performance and its mechanism of TiC/Inconel 625 composites prepared by laser metal deposition additive manufacturing](#)

J. Laser Appl. **27**, S17005 (2015); 10.2351/1.4898647

[Femtosecond laser post-processing of metal parts produced by laser additive manufacturing](#)

J. Laser Appl. **25**, 052009 (2013); 10.2351/1.4824146



Invited Review Article: Review of post-process optical form metrology for industrial-grade metal additive manufactured parts

P. I. Stavroulakis and R. K. Leach

Manufacturing Metrology Team, Faculty of Engineering, University of Nottingham, Nottingham, NG7 2RD, United Kingdom

(Received 10 November 2015; accepted 17 February 2016; published online 6 April 2016)

The scope of this review is to investigate the main post-process optical form measurement technologies available in industry today and to determine whether they are applicable to industrial-grade metal additive manufactured parts. An in-depth review of the operation of optical three-dimensional form measurement technologies applicable to metal additive manufacturing is presented, with a focus on their fundamental limitations. Looking into the future, some alternative candidate measurement technologies potentially applicable to metal additive manufacturing will be discussed, which either provide higher accuracy than currently available techniques but lack measurement volume, or inversely, which operate in the appropriate measurement volume but are not currently accurate enough to be used for industrial measurement. © 2016 AIP Publishing LLC. [<http://dx.doi.org/10.1063/1.4944983>]

I. INTRODUCTION

Metrology is a critical tool for manufacturing as it provides the necessary feedback for process control and post-process troubleshooting. Without fast and accurate metrology, setting up production procedures and maintaining production tolerances to minimise scrap parts is not possible. Metrology is especially important in the field of additive manufacturing (AM) where, in order to scale up production, multiple machines are used on the same manufacturing floor. Each machine can be considered as being an independent manufacturing process or manufacturing line that needs process feedback in order to achieve tight tolerances on the products being manufactured.

AM has recently been the focus of an ever-increasing number of studies conducted by government agencies,^{1–4} national measurement institutes,^{5,6} and commercial interest groups,^{7,8} and it is being described as one of the new emerging technologies which will transform the manufacturing sector in the future. The 2014 Wohler's market report has forecasted that the AM market will grow from 3.07×10^9 in 2013 to over 7×10^9 in 2016, and that the current market penetration is only about 8%; indicating that there is still a long period of potential growth for the market ahead.⁹ The international interest in AM, and the recognition that it is going to be pivotal to the future of manufacturing, has prompted multiple nations to promote collaboration between their AM industry and academic institutions via the creation of AM-specific technology centres, which will put these nations in a competitive position to take advantage of future AM markets. Examples of such centres can be found in the UK (Manufacturing Technology Centre), USA (America Makes Institute), and Australia (Advanced Manufacturing Cooperative Research Centre).

In this review, focus will be placed on form metrology, defined here as the determination of the external shape of an object, for metal AM products. Form metrology is critical

for quality control of AM products, and for AM machine manufacturers to successfully characterise and optimise their AM processes, when new materials and part geometries are developed. Shape deformation is one of the most noticeable effects following most metal AM processes due to the relaxation of thermal stresses^{10–12} and hence detailed *in situ* and post-process characterisation methods would be highly beneficial in understanding and contributing to the aversion of these effects. There are, of course, many more considerations beyond the part's form that need to be taken into account before an AM product can be used as a functional component in many applications. The product will also have to conform to various other tolerances related to the part's internal defects^{13,14} and surface texture,^{13–15} all of which are critical to its long-term functionality and industrial applicability. However, this review will only focus on external form measurement. Tolerances on form geometry vary from industry to industry, as do the requirements on the AM parts produced.¹⁶ This review will concentrate on the state-of-the-art in non-contact 3D optical metrology applicable to AM industries that have stringent product qualification standards, for example, in the aerospace and automotive industries. Contact systems, such as mechanical probe-based coordinate measuring machines (CMMs), have been used in such industries for many years,¹⁷ and can measure form to high accuracy (usually more accurately than current non-contact systems), but are relatively slow, not ideal for in-line inspection and only measure a limited number of points on an object's surface.¹⁸

The field of non-contact form metrology has been actively developed for many years under the colloquial terms of “machine vision” or “computer vision,” due to the fact that it was initially used in the areas of robotics and scene reconstruction. Recently, the computing power, algorithms, and hardware used have become faster and more sophisticated, and have allowed these systems to be used in metrology, providing measurements often in real time.^{19–24}

II. GENERAL OVERVIEW OF OPTICAL FORM MEASUREMENT SYSTEMS

Commercially available form measurement systems have seen a significant improvement in accuracy and precision, and many instrument suppliers are marketing their products for use specifically in quality control and post-process verification of machined parts in multiple manufacturing industries. Optical form measurement systems can generally be grouped into two families: passive and active.²⁵ Passive systems do not require spatiotemporal modulated illumination to operate, but do require a specific level of static ambient light as they are mostly based on photography. Most passive systems use one or multiple cameras, and image processing, to recreate the 3D form from a series of correlated images. Active systems use their own light sources to either raster scan or spatiotemporally vary the illumination of the surrounding environment. Active systems can recreate a 3D model of the object's form by detecting the modulation of projected illumination caused by the object's shape. A list of the most common techniques used for active and passive form measurement is given in Table I.

The advantages of passive over active systems are that they are usually cheaper in terms of hardware requirements, lower in mass, more compact, and hence easier to use. However, passive systems tend to be less accurate and slower compared to most active systems, as they rely on more complicated post-processing algorithms.²⁵ Additionally, various assumptions are usually made in passive systems about the object being measured; the most notable of which are the following:

- The object's surface always causes Lambertian reflectance. This assumption introduces errors when optically smooth or transparent surfaces are measured.²⁷
- The object's form is continuous without abrupt steps and discontinuities. This assumption is equivalent to low-pass filtering of high frequency components. The most common manifestation of this filtering effect is the rounding of sharp edges and removal of thin structures from the reconstruction.²⁷

TABLE I. Classification of active and passive 3D form measurement techniques.²⁶ Adapted with permission from Sensors **9**, 568 (2009). Free open access copyright under the Creative Commons License (CC BY v4.0) by the MDPI (Multidisciplinary Digital Publishing Institute).

3D form measurement technique	Passive	Active
Laser triangulation		X
Structured light		X
Stereo vision	X	
Photogrammetry	X	
Time of flight		X
Interferometry		X
Moiré fringe range contours		X
Shape from focusing	X	X
Shape from shadows		X
Texture gradients	X	
Shape from shading		X
Shape from photometry		X

- The idealised projection models, such as the ideal pinhole projection and orthographic projection, are good enough to approximate real measurements. This assumption manifests in reduced accuracy during reconstruction, as the non-ideal nature of real camera systems may not be taken into account.²⁷

The above assumptions are routinely used to make the determination of the object shape a more “well posed” problem (i.e., one that has a unique solution) and hence make the computational requirements for reconstruction simpler and the measurement process faster. However, these assumptions also reduce the accuracy of reconstruction to a level that restricts the ability of passive systems to perform high-accuracy form metrology.

Another advantage of active systems is that they overlay their own source of illumination onto the object so that they do not need the object being measured to have a textured surface in order to deduce its form, unlike passive systems.²⁵ Passive systems require textured surfaces in order to determine common features and hence relate multiple images taken at different positions on the object.²⁵ The process of associating common pixels between multiple images is the so-called “correspondence problem,” which is greatly simplified in active systems. In active systems, the images are not related by searching for common features between them but by using the overlaid illumination to achieve correspondence.²⁵ Hence, most high-precision optical form measurement solutions in the industrial market today, where high accuracy and reasonable speed are required, are active systems.

Active optical form measurement systems can be broadly categorised according to the accuracy they provide and the distance over which they operate, as shown in Figure 1. According to Ref. 25, five general families of active form measurement systems exist:

- Interferometry and confocal.
- Conoscopic holography.
- Triangulation via laser and white light projection.
- Time of flight (phase-based).
- Time of flight (pulse-based).

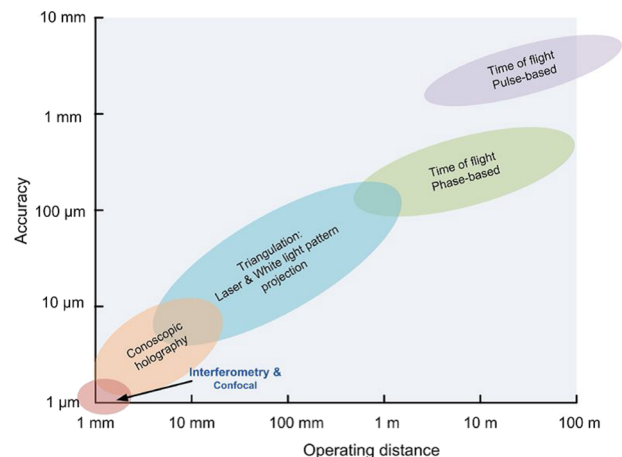


FIG. 1. Classification of active optical techniques in terms of range and accuracy (from Ref. 25). From S. Se and N. Pears, 3D Imaging, Analysis and Applications. Copyright 2012 Springer. Reproduced with permission from Springer. Her Majesty the Queen in Right of Canada.

TABLE II. Typical measurement requirements for aerospace and industrial applications.

Characteristic	Value used	Source
Maximum volume of measurement area (distance)	Up to (2000 × 2000 × 1500) mm	Recommended by VDI/VDE 2634-1 standard on industrial non-contact 3D scanning ²⁸
Dimensional tolerance	Varies with industry, typically ≤ 100 μm (±50 μm)	As per ¹⁶
Resolution and accuracy	As high as possible, typically ten times better than the tolerance range in order to provide adequate measurement confidence interval and appropriate process control.	N/A
Measurement time	As fast as possible, typical requirement is to be faster than the manufacturing process itself.	N/A

To select the appropriate active form measurement system for metal AM, the performance of different optical form measurement systems (Figure 1) has to be associated to the current industrial requirements shown in Table II and Figure 2.

The automotive and aerospace industries usually require tolerances in the range of hundreds of micrometres (Figure 2), at operating volumes of up to 2 m (Table II). These requirements (Figure 1) are theoretically achievable with current non-contact optical form measurement systems in ideal laboratory conditions, via laser triangulation and structured light systems. However, their applicability in terms of industrial requirements, which include a wide variety of surface textures (roughness, material optical properties), working environments (vibration, temperature, signal noise), high measurement speeds (in-line manufacturing, *in situ* measurements), and geometries (slope angles, aspect ratios, deep holes) poses a large challenge for these systems which needs to be addressed before their successful deployment is possible.

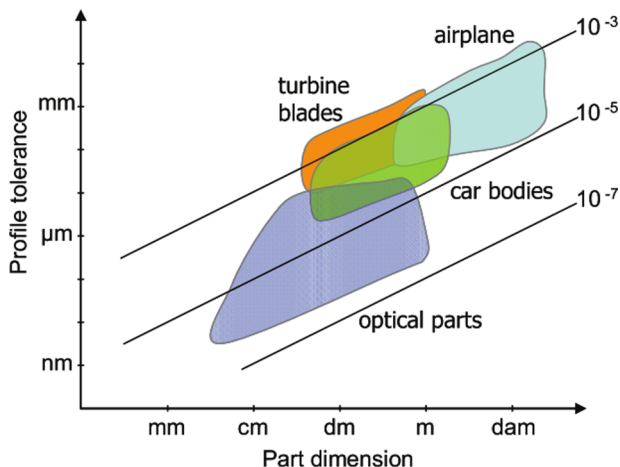


FIG. 2. Tolerance against part dimension for various industrial applications.¹⁶ Reprinted with permission from E. Savio, L. De Chiffre, and R. Schmitt, CIRP Ann.–Manuf. Technol. 56, 810–835 (2007). Copyright 2007 Elsevier.

A. Constraints introduced to form metrology from the nuances of metal AM

Further to matching the performance of optical form measurement systems to current metrological industrial requirements (Table II), the specific nuances of metal AM should be taken into account. The new challenges that metal AM brings to form metrology compared to traditional manufacturing are shown in Table III.

1. Surface texture

Optically rough surfaces, such as those found on parts created by metal AM, can be measured with currently available form measurement technologies, namely, laser triangulation and structured light systems, because these technologies rely on diffuse reflectance for their correct operation. The performance of laser triangulation and structured light systems in terms of signal-to-noise-ratio (SNR) is improved on parts made with optically rough surfaces compared to parts made via classical machining routes (subtractive manufacturing), which often have smoother surfaces and thus produce specular reflectance.

The specific type of surface texture produced in metal AM varies and depends highly on the process parameters and the method used to create the part. To illustrate this, an example between two different metal AM methods, laser sintering and laser melting, is shown in Figure 3. The surface texture in laser sintering is of the scale of the particle size used (in this case 22 μm–53 μm¹⁵) whereas in laser melting the surface texture is smoother but still contains large ridges and voids, and “as-printed” parts could also contain surface-sintered particles (Figure 3). In conclusion, the surface texture that is currently produced by metal AM is not optically smooth with respect to the specific measurement wavelengths used to investigate them (Refs. 15, 29, and 30) and hence measuring “as-printed” parts is usually less of a challenge to optical form measuring systems in terms of the higher SNR returned from the object. This does not mean that the roughness does not pose a

TABLE III. Constraints introduced by metal AM to form metrology via optical form measurement systems.

Constraint type	Constraint	Reason
Surface texture	Diffuse reflectance (an example of a flat surface created via a selective laser melting metal process is shown in Figure 3).	Typical surfaces produced via layering and powder based metal AM manufacturing technology are not optically smooth to visible wavelengths. ^{15,29,30}
Form geometry	Freeform, multiple occlusions, and shadows exist.	Little restriction in created geometry permits for complicated shapes with large number of discontinuities and line of sight occlusions present.
Material range	Appreciable variation of absorption/reflection properties between different materials.	Inhibits the overlay of specific wavelengths, more important for laser triangulation than structured light.

measurement challenge on the accuracy of the final result,¹⁵ especially when the roughness is too fine to resolve.³¹

Many manufacturers, however, use various post-processing steps and standard subtractive manufacturing techniques to polish some if not all of the surfaces of metal AM parts in order to make them functional and reduce surface stresses in order to avoid the formation of microcracks, which can lead to long-term part failure.³³ Another reason for subtractive post treatment is to achieve tight dimensional tolerances not achievable by AM alone. Hence, although the “as-printed” rough surfaces are relatively simple to measure, the need to measure smooth surfaces produced by post-processing metal AM parts poses a challenge for measuring the form of a finalised metal AM product.

2. Freeform geometry

The freeform geometry used in metal AM (and AM in general) involves the frequent presence of occlusions and high slope angles. Current optical form measurement systems have inherent limitations due to their requirement to work in line-of-sight and ideally not at angles too far from that of normal incidence to the object. Hence it is difficult for them to measure complex geometric structures from a single measurement position.

However, these complications can be partially alleviated through data fusion of multiple measurements taken from different viewpoints.³⁴ Fusing data from different viewpoints in a cost-efficient way would, however, require the develop-

ment of mechanical positioning systems in order to move around the illumination and image sensing elements (laser, camera, and projector) and allow the complete part to be scanned quickly and efficiently. Adding sensor motion and fusion of measurement data will inevitably result in an increase of measurement uncertainty for the whole system. To keep the uncertainties added to low levels, both the positioning system and algorithms used must be highly accurate.

3. Material range

Currently, the most popular material investigated for use in AM is the titanium alloy Ti6Al4V, as it is commonly used both in the medical and aerospace industries.³⁵ The main reason for the focus on AM is that this titanium alloy is relatively expensive and hence being able to use AM would minimise material scrap and provide large cost savings to these industries, hence outweighing the drawbacks and costs of changing their process to AM. However, many other metals are also under investigation for AM, as shown in Table IV, and more materials and alloys are continuously added to this list as more innovative uses of AM are investigated.

Any generalised post-process metrology system aspiring to be used for characterising metal AM products would need to take into account the wide range of materials that are attracting commercial interest and be able to account for the alloys currently under research. In terms of form measurement systems, this means paying attention to the spread of optical properties of the materials currently used for AM (i.e., making

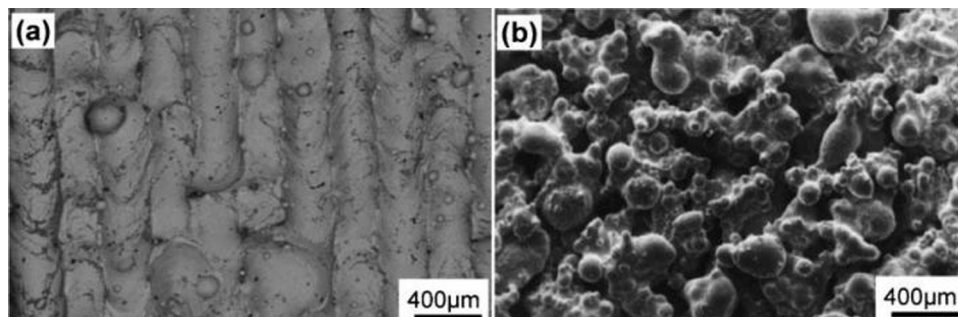


FIG. 3. Laser melted (a) and laser sintered (b) metal AM morphologies.³² Reproduced with permission from D. D. Gu, W. Meiners, K. Wissenbach, and R. Poprawe, *Int. Mater. Rev.* **57**, 133 (2012). Copyright 2012 The Institute of Materials, Minerals and Mining reprinted by permission of (Taylor & Francis Ltd, www.tandfonline.com) on behalf of The Institute of Materials, Minerals and Mining.

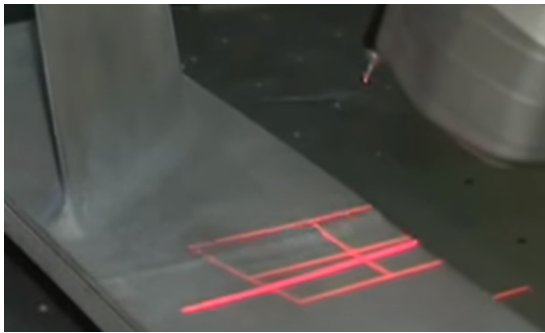


FIG. 4. Articulating arm laser line scanning of a turbine blade. (Reprinted from source: Martin Dury, NPL's National Freeform Centre.)

sure the power or wavelength of the light used is adequate to characterise the wide range of alloys and metals) or at least to be able to provide different optical configurations to deal with the spread.

III. IN-DEPTH COMPARISON OF OPTICAL NON-CONTACT FORM MEASUREMENT SYSTEMS CURRENTLY MOST APPLICABLE TO AM

As discussed in Section II, the two main types of optical form measurement systems which would be most useful for industrial AM are those currently used in conventional manufacturing industry, namely, laser triangulation and structured light projection. These two types of systems have the accuracy and the measurement volume required by demanding industries, such as automotive and aerospace, but need to be able to satisfy the nuances of metal AM, such as optically rough surface texture, freeform geometry, and the wide range of materials used. A more in-depth analytical explanation of the techniques along with an investigation of their limitations will be presented hereafter.

A. Laser triangulation

Laser triangulation systems project a laser spot or a line onto the part (Figure 4). The spot or line is then scanned across the object by deflecting the beam using a mirror. At each mirror position, triangulation is performed to calculate the height of the scanned points.

The triangulation principle used for the measurement of the distance between the laser and the object at each point is shown in Figure 5. Light from a laser strikes the surface and is registered at a specific point on the CCD detector. If

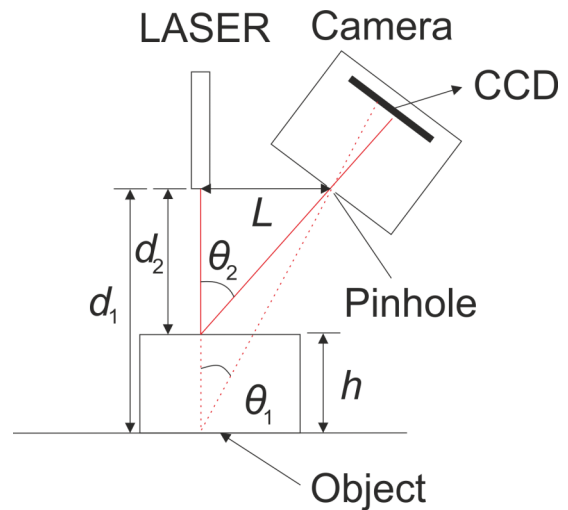


FIG. 5. Principle of laser triangulation.

the distance between the object and the laser changes from d_1 to d_2 , the angle between the laser and detected reflection will also change from θ_1 to θ_2 . The change of angle will cause the laser spot to register at a different point on the CCD and this difference can be used to calculate the height at each point.

In the example shown in Figure 5, the distance between the laser and the object is given by

$$d_2 = L \tan(90 - \theta_2), \tag{1}$$

where d_2 is the distance between the laser and the object, θ_2 is the angle between the incident and reflected beams, and L is the distance between the CCD photodetector and the laser.

In order to extract the actual height of the measured point h , the overall distance between the laser and the measurement platform d_1 needs to be measured and known beforehand ($h = d_1 - d_2$).

Four configurations of laser and camera are available for a laser triangulation system:³⁸ “Reverse ordinary,” “Ordinary,” “Specular,” and “Look-Away,” shown in Figure 6. The resolution of the system is affected by the orientation of the system as is the susceptibility to occlusions and the laser power required to get an unsaturated image with high SNR.³⁸

1. Calibration

Laser triangulation systems require calibration in order to minimise errors due to the variation of the projected angle and height of the laser beam after its reflection from a freeform object,³⁹ the change in reflected intensity over different object heights³⁸ and the non-idealities of the optical system (such as lens distortions, the laser line, and vision plane parameters). The calibration process requires linear and non-linear optimisation of re-projection errors.⁴⁰ The calibration of the measurement device is usually achieved by measuring traceable reference objects.^{38,40} Another method that is used for calibration is to move a flat plane through the measurement range and compare the range results from the laser triangulation system to those of a more accurate measurement technique, such as a laser interferometer which is used to measure the same plane

TABLE IV. Selected materials commercially used in AM processing, from Ref. 36. With kind permission from W. E. Frazier, J. Mater. Eng. Perform. 23, 1917 (2014). Copyright 2014 Springer Science + Business Media, Table II.

Titanium	Aluminium	Tool steels	Super alloys	Stainless steel	Refractory
Ti-6Al-4V	Al-Si-Mg	H13	IN625	316 and 316L	MoRe
ELI Ti	6061	Cermets	IN718	420	Ta-W
CP Ti			Stellite	347	CoCr
γ -TiAl				PH 17-4	Alumina

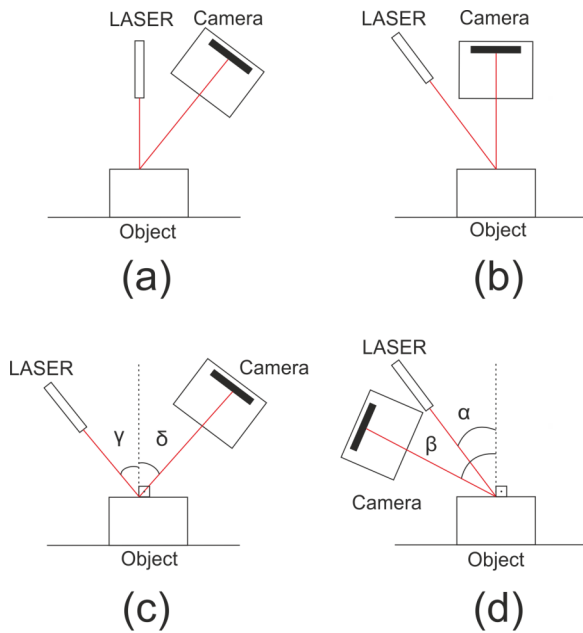


FIG. 6. Four types of laser triangulation setups: (a) “Reverse ordinary,” (b) “Ordinary,” (c) “Specular,” and (d) “Look-Away.” Angles shown in all cases are non-identical (i.e., $\alpha \neq \beta$, $\gamma \neq \delta$).

simultaneously.⁴¹ Relative accuracies of 1 part in 3400 of the measurement range have been reported when using a visible target to calibrate the CCD sensor.⁴⁰

2. Sources of uncertainty in laser triangulation

The sources of error in laser triangulation systems are associated with the fundamental uncertainty in the position of the centroid of the spot. A collection of the main sources of error with respect to intensity is shown in Figure 7.

The most fundamental (albeit not always most dominant) source of measurement uncertainty in laser triangulation, which ultimately limits the instrument’s accuracy and cannot be completely eliminated, is the roughness of the surface. As the surface becomes “optically rough” (defined here as when the height of the features becomes comparable to the quarter of the incident wavelength), speckle noise arises due to Raleigh, or coherent, scattering. The equivalent height uncertainty due to speckle noise is given by^{42,43}

$$\delta x = \frac{\lambda_0}{2\pi \sin(\theta) \sin(u)\sqrt{N}}, \tag{2}$$

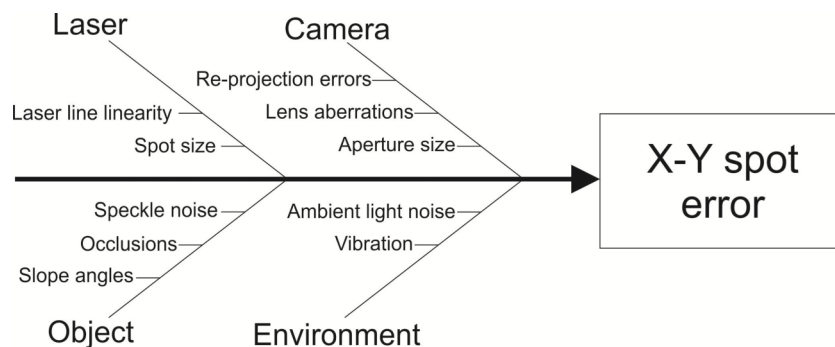


FIG. 7. Ishikawa or “fishbone” diagram that summarises the main sources of uncertainty in laser triangulation.

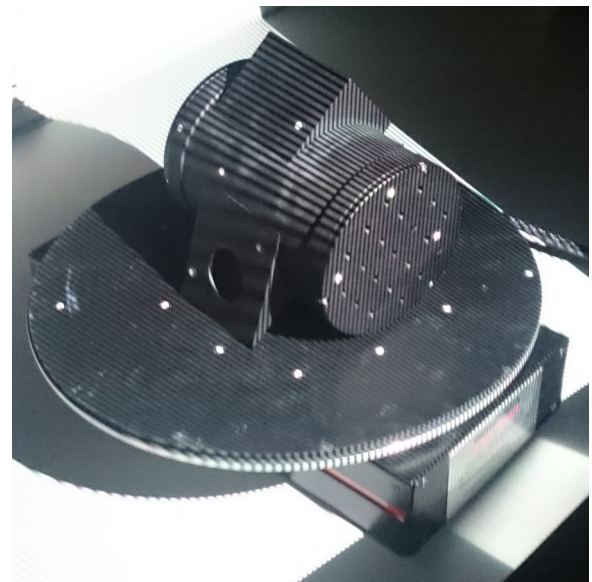


FIG. 8. Image of structured light fringes projected onto mechanical part. The part was supplied by MetrixNDT.

where θ is the triangulation angle, u is the aperture angle at the detector, λ_0 is the source wavelength, and N is the number of photons.

Finally, the speed of laser triangulation depends on the resolution required, since the measurement cycle increases linearly with the number of measurement points required.

B. Structured light projection techniques

Areal light codification via structured light can be achieved by projecting either binary or continuously varying signals onto a surface. In the case of binary signals, correspondence is extracted by comparing the temporal and spatial patterns extracted through various structured light schemes, for example, binary coding,^{44,45} M-array,^{44,45} N-ary codes,^{44,45} and multi-level Gray coding^{44,45} (Figure 8).

In the case of continuously varying signals, such as sinusoidal fringe patterns or trapezoidal fringe patterns,⁴⁶ correspondence is not necessary as the absolute phase of each point is extracted by retrieving an analytical solution. For other continuously varying signals, such as linear intensity-ratio or “wedge” patterns,⁴⁷ correspondence is found by comparing the pixel intensity to a look-up table. Due to the continuity

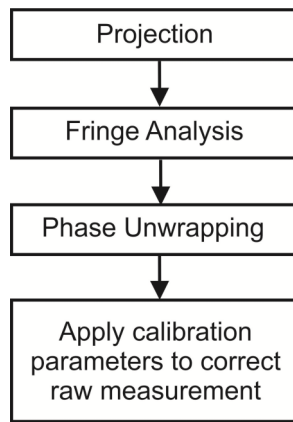


FIG. 9. Flow chart of fringe projection methods.

of the projected signal, continuously varying signals can usually achieve pixel-level resolution at the detector since the height information can be calculated analytically, after unwrapping and/or scaling of the received information at each pixel.⁴⁴

Sinusoidal fringe projection is one such “continuous” technique, which can provide high accuracy and dense point mapping through extraction of the angular phase of the projected pattern from every pixel in the image deterministically, by projecting at least three phase-shifted versions of the same sinusoidal pattern.⁴⁸ Considering all the state-of-the-art structured light techniques, sinusoidal fringe projection seems to hold the most promise for industrial applications as it can operate with high speed (requires only three phase-shifted projections), has pixel-level resolution, and has been shown to achieve the highest accuracy in a recent review which performed a study of the same object using different structured light techniques.⁴⁴ The general measurement flow for fringe projection methods is shown in Figure 9.

A minimum of three phase-shifted images per view are required⁴⁸ to extract the phase per pixel analytically, because the description of the phase of each pixel has three unknowns. Equations (3)–(5) describe the illumination per pixel for three $2\pi/3$ radian phase-shifted images:⁴⁸

$$I_1(x, y) = I_b(x, y) + I_a(x, y) \cos(\phi(x, y) - \frac{2\pi}{3}), \quad (3)$$

$$I_2(x, y) = I_b(x, y) + I_a(x, y) \cos(\phi(x, y)), \quad (4)$$

$$I_3(x, y) = I_b(x, y) + I_a(x, y) \cos(\phi(x, y) + \frac{2\pi}{3}), \quad (5)$$

where I_1 , I_2 , and I_3 are the intensities detected at the CCD pixel for each of the three phase shifts, I_a is the contrast between fringes, I_b the background noise, and $\phi(x, y)$ is the phase of the projected pattern. The phase per pixel can be calculated by solving Equations (3)–(5) for the phase term and hence the relationship that results for the phase per pixel in the image is given by²¹

$$\phi(x, y) = \tan^{-1} \left(\sqrt{3} \frac{I_1(x, y) - I_3(x, y)}{2I_2(x, y) - I_1(x, y) - I_3(x, y)} \right). \quad (6)$$

Alternative versions of sinusoidal fringe projection, which attempt to perform phase information extraction using a single

frame of projected fringes (often called “one-shot” methods) via various colour and fringe multiplexing techniques have been developed and are described elsewhere.⁴⁹ The use of colour in sinusoidal fringe projection, however, adds to the complexity of detecting the fringes at the detector and increases the sensitivity of the image to environmental light intensity and object colour noise.⁴⁹ The boundaries between colour strips have to be accurately identified and this increases the difficulty in separating colour noise from the overlaid pattern in natural light situations, especially if the colour of the object surface varies over its volume.

1. Alternative phase retrieval techniques

“One-shot” schemes, which acquire the phase information from a single black and white sinusoidal fringe image, use simple Fourier analysis,⁵⁰ windowed Fourier analysis,⁵¹ or wavelet transforms^{52–54} to achieve phase extraction. The success of these techniques hinges on the ability to filter the frequency domain correctly, which requires the projected fringe frequency to be clearly distinct from all other spatial frequencies present in the image, especially for the simple Fourier analysis technique.⁵⁰

If the frequency of the overlaid pattern cannot be clearly distinguished from other spatial frequencies present in the image, more uncertainty is added to the measurement of phase. Additionally, although single-frame phase estimation may allow for faster phase extraction, in post-process form metrology achieving video-rate 3D imaging speed is often less critical than accuracy.

2. Unwrapping

Due to the 2π wrapping of the inverse trigonometric function (Equation (6)), the conversion between phase difference and absolute phase includes 2π discontinuities. Therefore, before the height can be retrieved via appropriate dimensional scaling of the phase angle, the 2π discontinuities must be removed.

For a continuous surface (a surface which has height discontinuities that are smaller than the equivalent 2π phase difference in the phase map), unwrapping the phase is a trivial problem as all of the discontinuities can be filtered out by identifying them and adding or subtracting 2π from the phase when a phase jump is detected in order to guarantee continuity. However, for structures that include large discontinuities, such as holes or steps that are greater than 2π in equivalent phase, simply adding or subtracting 2π when a phase jump is detected is not possible. Multiple strategies have been developed and are available to assist with unwrapping the phase in fringe projection, the most common of which use binary codes⁵⁵ or multiple spatial wavelengths.⁵⁶

3. Optical calibration of projector-camera system

The calibration of the distortions present in fringe projection is an important step required to compensate for system non-ideality. The two main corrections which are required to

successfully translate the intensity values in the phase map into real height values with high-accuracy are the gamma⁵⁷ and the optical distortions.⁵⁸ Relative accuracies of 0.01% have been shown to be achievable in sinusoidal fringe projection when correcting for both optical and gamma distortions.⁵⁹

There is a large variety of techniques which can be used to calibrate for projector-camera system optical distortions, such as using pre-calibrated cameras to assign projector correspondences,^{60–62} varying the projected pattern by changing projector position,^{63–65} performing an iterative adjustment of projected pattern to overlap a printed pattern,^{66,67} or moving a flat surface through the measurement volume via a moving stage.⁶⁸

Different types of algorithms can be used to perform the calibration, such as homography transformation between the calibration plane and the projector image plane,^{64,66,69} computation of projector point correspondences from images captured by the camera by creating artificial images at the projector resolution,^{63,69} or computation of projector point correspondences from images captured by the camera directly.⁷⁰

When the correspondences of the system are known, the projector-camera system can be calibrated with any of the well-established techniques used for a two-camera stereo system by assuming the projector is an inverse camera.⁷⁰ In this case three types of general approaches exist:

- Using a reference object of known shape/size.⁷⁰
- Self-calibration techniques.⁷⁰
- Hybrid photogrammetry/self-calibration techniques.⁵⁸

4. Projector gamma calibration

For binary structured light signals, correcting for projector gamma is less important as the exact illumination level is not critical to the measurement. Since the measurement involves determination of binary thresholds between “dark” and “bright” pixels, the noise tolerance is much larger compared to continuous structured light techniques.⁷¹

However, for “analogue” or “continuous fringe” techniques, gamma is significant, as the exact intensity level detected is critical to the accuracy of the phase extraction. A large number of techniques have been used to correct for the projector gamma through use of neural networks,⁵⁷ statistical

analysis,⁷² Fourier spectrum analysis,⁷³ look-up tables,⁷⁴ and iterative phase compensation algorithms.⁷⁵

5. Sources of uncertainty in sinusoidal fringe projection

The main sources of uncertainty in determining the phase of a fringe projection system have to do with errors that affect the exact value of the intensity in the detected image. An error in intensity will influence the phase value calculated (given by Equation (6)) and ultimately, the height information extracted. The main sources of error with respect to intensity are shown in Figure 10. Most significantly, the intensity recorded on the CCD can be affected by projector issues such as temporal intensity variations (for example, lamp warmup time⁷⁶), uncorrected gamma,⁷² and the limited resolution used to project high-quality continuous signal and lens distortions. As far as the camera is concerned, the factors that can play an important role in the variation of the expected intensity are the variable dark pixel noise, shot noise, limited dynamic range, and distortions from the optics. The object may have different regions of varying texture or colour that scatter light differently thus registering as different intensities on the detector even though the regions are equal in height. Reflective surfaces may saturate the detector so that the overlay of a pattern may not be feasible. In the ambient environment, there may be varying light noise or indirect reflection changes, induced by the vibration of the structured light system or the object, that may affect the intensity.

IV. OVERVIEW OF FUTURE CANDIDATE FORM MEASUREMENT TECHNOLOGIES FOR ADDITIVE MANUFACTURING

Looking into the future of form measurement, the next generation of systems applicable to the metal AM industry could originate from a variety of different sources. Firstly, the most obvious source would be the improvement of the algorithms or hardware currently used in laser triangulation and structured light systems to allow for higher accuracies and faster operation. Alternatively, high-resolution short-range techniques, used mostly for surface texture measurement, could be made to operate over the ranges required in AM

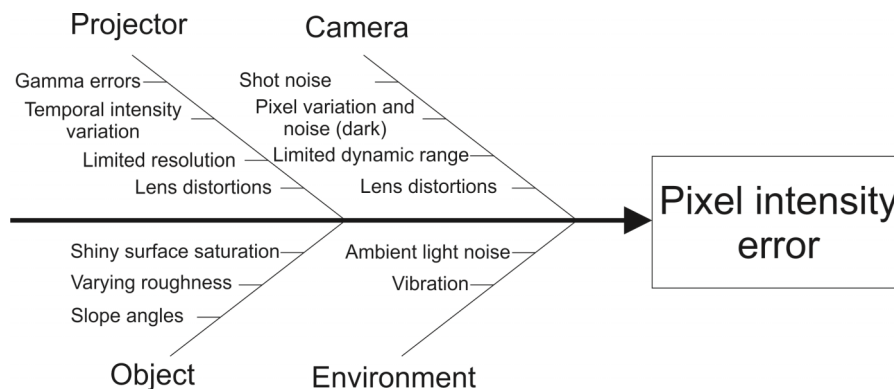


FIG. 10. Ishikawa or “fishbone” diagram that summarises the main sources of uncertainty identified in sinusoidal fringe projection.

manufacturing. Moreover, the next generation of form measurement technologies for AM may be developed by improving the accuracy and precision of low-resolution long-range techniques (for example, time-of-flight, photogrammetry) which are currently used for large-scale topographic surveying.

Section III presented a detailed comparison of two established metrology methods that have been demonstrated to perform well on typical metal AM surfaces. In this section, a summary of the most promising metrology methods, which could be the basis for the new generation of metal AM form measurement technology, will be presented. The methods described are either novel in of themselves or currently undergoing rapid development and have the potential to be useful for metal AM in the future. At the end of this section, a comparison of reported ranges and accuracies for all the techniques mentioned will also be performed.

A. Active focus detection through shear interferometry

Confocal focus detection systems (Figure 11) analyse the curvature of the reflected wavefront via shearing interferometry and hence are able to detect the distance from which a wavefront has been reflected by calculating the distance of the centre of curvature from the sensor. This technique has been shown to achieve a distance resolution of $10\ \mu\text{m}$ at 300 mm from the instrument on smooth specular surfaces and a resolution-to-distance ratio of 1:5000 for diffusely reflecting objects.⁷⁷ The variation of accuracy on the type of surface texture makes the technique less attractive for high-accuracy form metrology, where surfaces are produced with highly variable surface texture depending on material and AM process parameters. Another limiting characteristic of active focus detection through shear interferometry for post-process AM is that it is an inherently point-to-point technique that requires scanning in both lateral directions of the object plane, and will be prohibitively slow for measuring relatively large parts.

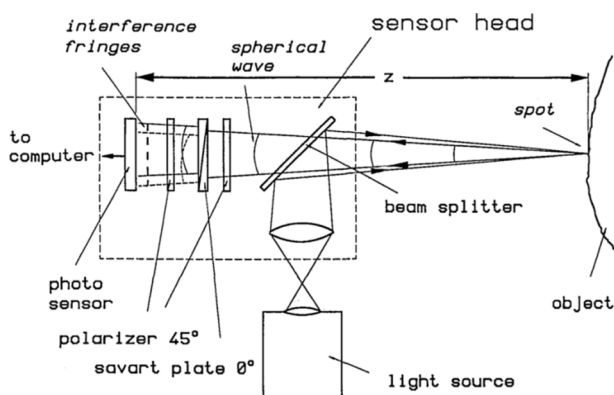


FIG. 11. Depth of focus determination via shear interferometry wavefront shape determination.⁷⁷ Reproduced with permission from G. Häusler, J. H. Less, M. Maul, and H. Weissmann, *Appl. Opt.* **27**, 4638 (1988). Fair Use under United States Copyright Law.

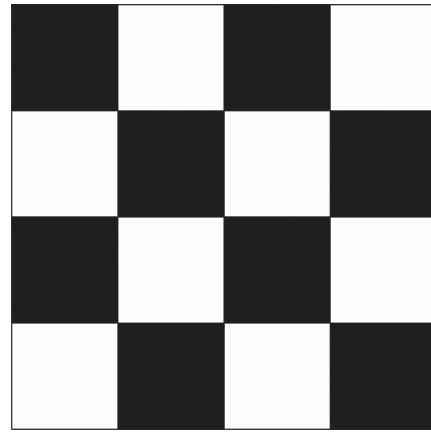


FIG. 12. Example of checkerboard-type pattern superimposed on 3D scene to overcome texture-less object problem.

B. Active shape-from-focus detection with the assistance of a projected pattern

In the technique described in Ref. 78 the classic method of shape-from-focus is used, whereby a camera takes images of the scene at different focal distances and for each image the in-focus regions are stored along with the focal distance information. The images can then be reconstructed into a 3D model by using the focal distance information. The difference between this method and simple shape-from-focus is the use of active projection patterns to improve the measurement. More specifically, the classical problem which is present in shape-from-focus techniques of ensuring shape recovery from smooth texture-less regions, where in focus and out of focus images appear similar, is solved by overlaying a projected pattern onto the object⁷⁸ (Figure 12). Problems which still limit the accuracy of the technique described in Ref. 78 are the need for accurate modelling of the optics and sensing elements, the issue of constant magnification defocusing and limited repeatability, thus active shape-from-focus detection is still some way from being applicable for industrial AM applications.

C. Projection Moiré profilometry

Moiré profilometry (also called out-of-plane Moiré),^{79–81} is an image-grating superposition technique where a set of black and white lines is projected onto an object. The deformed image that results is demodulated by superimposing it to a copy of the original projected image at the receiver to extract the Moiré interferogram. The resulting Moiré interferogram represents contours of equal phase difference which correlate to height contours through use of a scaling factor and can be used to reconstruct the 3D image.⁸² There are several types of out-of-plane Moiré, which are used for profilometry, for example, shadow Moiré, projection Moiré, and reflection Moiré, depending on where in the optical chain the patterns are placed. In projection Moiré a copy of the pattern is placed both in front of the projector and camera of the system (Figure 13), in reflection Moiré, one pattern is placed around the aperture of the camera and the diffuse light source is placed behind the camera and in shadow Moiré, one pattern is placed very near

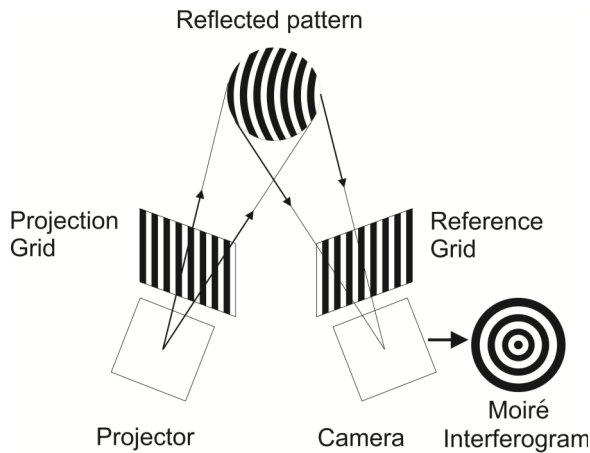


FIG. 13. Schematic diagram of projection Moiré profilometry. Light is deformed by the object profile and translated into height contours by observing it through an identical grating superimposed on the camera.

the sample which when tilted or moved interferes with its own shadow upon reflection. The most applicable type of Moiré for 3D contouring of large objects is projection Moiré, as the other two types are usually used for measurement of small out-of-plane deformations.

Projection Moiré (Figure 13) can be performed in different ways depending on the manner in which the reflected pattern is superimposed to the reference pattern to create the Moiré interferogram and extract the phase map. These include optical Moiré,⁸⁰ digital Moiré,⁸³ and Fourier Moiré.⁵⁰ Optical Moiré is the classical “analogue” version whereby a photographic plate is exposed twice with a combination of both the pattern’s image on the object and a copy of the original unmodulated fringe pattern. The invention of digital imaging and fast computer processing enabled digital Moiré in which only the image of the pattern projected onto the object needs to be captured, as the original pattern can be “digitally superimposed” when post-processing the image. Digital Moiré removes the need for an optically superimposed pattern at the detector (as required in optical Moiré). One of the disadvantages of digital Moiré is that the digital grid is of limited resolution and thus requires grid filtering to be implemented in order to remove the effect of image pixelation. Additionally, in order to achieve high resolution, very dense grids need to be used,⁸² so there is a trade-off between resolution and object size.

The Fourier Moiré technique⁵⁰ is another digital technique that also does not require the fringe pattern to be optically superimposed but, unlike digital Moiré, it does not require the digital superposition of the pattern. Fourier Moiré selects the range of spatial frequencies of the image around that of the projected fringe pattern carrier frequency by applying appropriate filtering to the Fourier transform of the captured image. This range of spatial frequencies around the carrier frequency (which are usually well separated from other frequency components in the image) represent the deformation of the fringe pattern due to the modulation of the pattern caused by the heights on the measured object. The carrier frequency is then subtracted and an inverse Fourier transform is performed to obtain the phase difference map for each pixel in the image. The phase difference is associated to the modulation caused

by the height of the object at each point by scaling.⁵⁰ The disadvantage of Fourier Moiré is that the low-pass filtering applied inevitably leads to high frequency image components, such as sharp steps, to either be ignored or smoothed out and, therefore, it has limited in-plane resolution.⁸² Additionally, the spatial frequency components of the fringe pattern need to be clearly distinct and not overlap with spatial frequencies that exist on the object.⁵⁰

D. Holographic profilometry

Holographic contouring (also called digital holographic profilometry, optical heterodyne profilometry⁸⁴) is a technique that uses wavefront reconstruction to deduce height. For optically smooth reflective surfaces, which are defined as surfaces where the roughness is not greater than a quarter of the incident wavelength, only one image is necessary to interpret the height information and the setup is similar to a Michelson interferometer,⁸⁵ whereas when optically rough diffusely scattering surfaces are involved (such as in metal AM), two holographic exposures with a change of either source location,⁸⁶ refractive index of the surrounding material,⁸⁷ or the wavelength of the illumination⁸⁸ are required. The basic setup required to perform holographic profilometry is as shown in Figure 14. The resulting interferogram is directly associable to the iso-height contours of the object.

Out of the three methods of creating the holographic interferograms, using a frequency shift is most popular as it is easier to apply in a practical system. Frequency shifting has been achieved by changing the injection current of a laser diode,⁸⁹ modifying the cavity length of a pulsed laser⁹⁰ or tuning a dye laser.⁹¹

E. Volume holographic profilometry

Volume holographic profilometry uses an exotic optical component known as a volumetric hologram, which is a

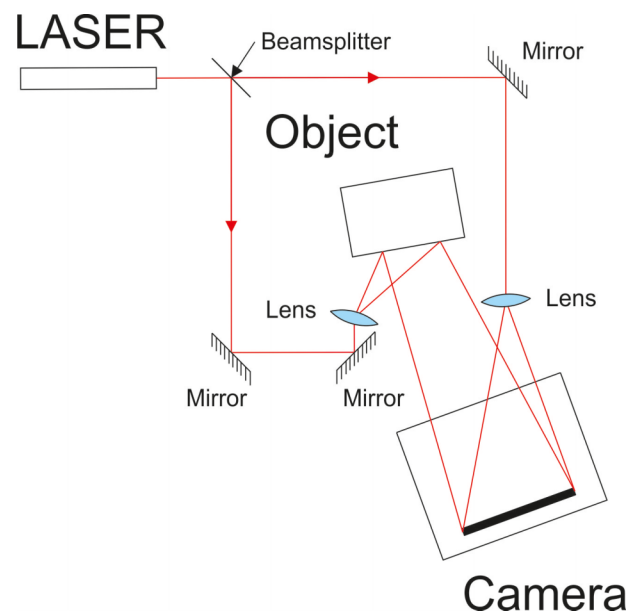


FIG. 14. Schematic of holographic interferometry.

photosensitive semi-transparent coloured material such as an alkali halide,⁹² in which holographic interference information can be inscribed in the form of Bragg gratings. Volume holographic profilometry exploits the Bragg angular sensitivity of incoming wavefronts in order to extract the depth information by either line scanning the volume hologram with a laser spot in the lateral and axial directions⁹³ or using a white light source to create a unidirectional spectral map overlaid on the object.⁹⁴ The major disadvantage of volume holographic profilometry is that in both cases the stage requires scanning in the height direction, which limits the range of measurement to that available by the scanning system and makes the procedure slow. Additionally, volume holographic profilometry has been shown to have poor depth selectivity due to the slow Bragg angle degeneracy of the incident beam.⁹⁵

F. Frequency modulated continuous wave ranging

Time-of-flight systems measure distance indirectly by reflecting a beam from the object and determining the time required for the beam to return to a detector. Time-of-flight systems are usually used for long-range measurements such as those required in topographical surveys. Recent developments in frequency-modulated continuous wave ranging sensors allow the technology to operate in a shorter range from the measured object (10 cm–50 cm) and with higher accuracy which enables their use in metal AM metrology. One such technique is described in Ref. 96. As shown in Figure 15 the reference signal is passed by a fibre optic cable to the splitter and is fed to each sensing element individually, whereby the measured signal travels out of the fibre, reflects off the object, and is multiplexed with the reference signal on each sensing

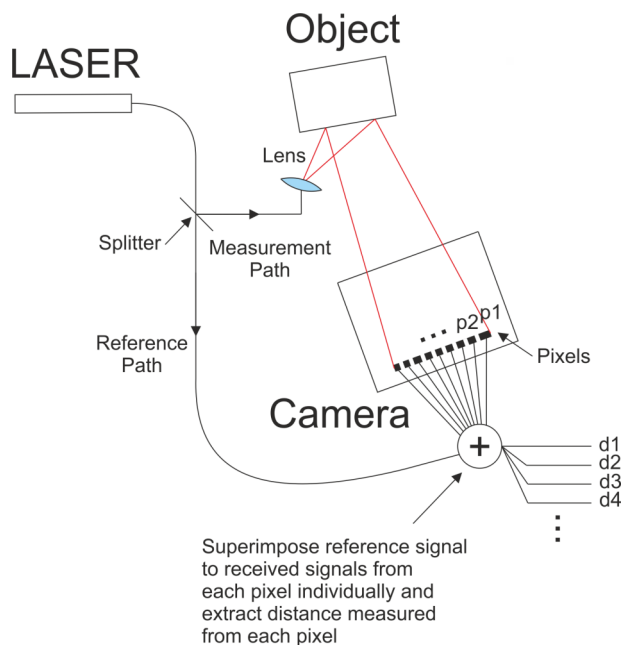


FIG. 15. Principle of FMCW (Frequency Modulated Continuous Wave) ranging. Time delay between a reference path and the light reflected from the object is measured for each pixel ($p1, p2$) resulting in the calculation of the path difference distance ($d1, d2$) from the object at each part of the CCD and hence the topography of the object.

element. The technology is still at a very low technology readiness level to be of practical use to AM metrology due to the limited resolution and high measurement complexity involved. Nevertheless, systems based on this principle have demonstrated 15 μm depth resolution and up to a 500 mm measurement range. This makes it a good contender to be the next form measurement technology for AM if the bottleneck of low resolution can be ameliorated.⁹⁶

G. Close-range photogrammetry

Photogrammetry⁹⁷ is a process whereby measurements (such as object position and shape) are extracted from multiple photographs. Most passive measurement techniques (i.e., stereo vision,⁹⁸ shape from shading⁹⁹) can be considered a subset or special case of photogrammetry, as they use multiple photographs to extract the data required from one or multiple images. Close range photogrammetry (defined as photogrammetry where the target is closer to the camera than 100 m) has been shown to be a viable method for precise and accurate measurements for metal parts.^{100,101}

The most significant drawback of close-range photogrammetry is the problem of correspondence between images (association of common pixels), which is usually solved by using set “targets.”¹⁰⁰ Targets are easily recognisable adhesive stickers that can be used to calculate the difference in camera position between photographs.¹⁰⁰ The use of targets is time-consuming and problematic for rapid metrology as the distribution of stickers is up to the discretion of the operator and has to be random enough to be unique so that the targets can be mapped, and ubiquitous enough so that there are enough common targets between scenes in order to track the movement of the camera in each image. Additionally, even though the accuracies reported for calibrated small objects (25 mm and 30 mm in diameter) are in the acceptable ranges (15 μm in accuracy with a 3σ standard deviation of 75 μm ¹⁰⁰), for larger objects the accuracies are predicted to be lower as the image resolution would also be lower.

H. Comparison between future candidate form measurement technologies for AM

The reported accuracies and measurement ranges (summarised in Table V) of the aforementioned measurement methods are perceived close to the industrial inspection requirements for automotive and aerospace (Figure 2). This is why they are considered to be good candidates for the next generation of metal AM provided they can be developed further and are proven in the field so that they can be adopted by industry.

V. HIGH-PRECISION SHORT-RANGE OPTICAL TECHNIQUES

Looking even further into the future, we can envisage even higher precision optical non-contact techniques required for specialized industries and demanding industrial applications. However, high precision optical non-contact techniques that operate with optically rough surfaces are normally used in a

TABLE V. Comparison of possible future candidate 3D scanning techniques.

Technique	Best dimensional resolution reported in height axis	Measurement range	Type of view	Works on optically rough surface
Active focus detection through shear interferometry ⁷⁷	10 μm (on optically smooth surfaces) resolution reduced for rough surfaces	300 mm	Point-to-point	Yes
Time of flight ⁹⁶	15 μm	500 mm	Full field	Yes
Close-range photogrammetry ¹⁰⁰	$\sim 15 \mu\text{m}$	30 mm–100 m ^a	Full field	Yes
Volume holographic profilometry ⁹⁵	$\sim 20 \mu\text{m}$ –2 mm	20 cm–2 m	Full field	Yes
Holographic profilometry ⁸⁴	10 μm	50 mm–300 mm depending on object reflectance	Full field	Yes
Moiré profilometry ¹⁰²	Typically $\sim 25 \mu\text{m}$ depends on grating frequency used	N/A	Full field	Yes

^aUsed definition of close range photogrammetry in the paper and size of object in the study to obtain estimates for range values because the distance between the camera and the object was not defined in the paper. The most likely distance from photographs shown is estimated to be 40 cm–50 cm.

TABLE VI. Comparison of three example high precision non-contact 3D measurement techniques that operate on rough surfaces.

Technique	Best dimensional resolution reported in height axis	Measurement range	Type of view	Works on optically rough surface
Coherence scanning interferometry ¹⁰³	<2 nm	Depends on piezo stage range, usually of the order of $\sim 100 \mu\text{m}$ ¹⁰³	Point-to-point or full field	Yes
Multi-wavelength (hyperspectral) interferometry ¹⁰⁵	80 nm	350 μm	Full field	Yes
Focus variation ¹⁰⁶	10 nm	3.2 mm–22 mm	Full field	Yes

microscope-style setup as they are very sensitive to vibration and non-laboratory conditions. Additionally, as mentioned in Section IV, these higher precision optical non-contact techniques usually have a very short working range and thus they are currently mostly applicable for surface measurement. Some examples of such systems include coherence scanning interferometry,¹⁰³ wavelength scanning interferometry,¹⁰⁴ multi-wavelength interferometry,¹⁰⁵ and high-accuracy focus variation,¹⁰⁶ which are summarised in Table VI. Such methods will not be further discussed here as they are not considered to be currently applicable for industrial AM form metrology due to their short working range and narrow field of view. Detailed reviews of such systems can be found elsewhere.³⁷

VI. CONCLUSIONS

AM does not in itself present entirely new measurement challenges. What it does do is present a level of complexity in geometry that is unprecedented in manufacturing. With the almost infinite design freedom comes almost infinite measurement complexity. Standard measurement procedures, tolerancing practices, and process control methods from “conventional manufacturing” cannot be easily ported across to this new manufacturing paradigm. Fundamental research is required to develop new metrology tools, new ways of using existing tools, new characterisation methods, and tolerance rules that can cope with the complexity inherent in AM.

Taking into account the optically rough surfaces of industrial metal AM parts, the typical object size, the measurement accuracy required for top-end industrial 3D measurement applications, and practical matters such as commercial availability and cost, the most applicable form measurement principles for metal AM have been found to be laser triangulation and structured light projection.

Even though both techniques use the outputs of CCD arrays to take their measurements, the fundamental source of uncertainty in the two techniques is somewhat different. Laser triangulation is based on the calculation of the angle between the projected and reflected laser beam path and has its fundamental source of uncertainty arising from the localisation of the laser spot centroid projected onto the CCD. Alternatively, sinusoidal fringe projection, which is based on the measurement of the phase difference between an observed fringe pattern and the projected pattern on a surface, relies on the accurate measurement of intensity at each pixel of the observed image. The uncertainty of localisation of the laser spot centroid in laser triangulation can be heavily affected by the roughness of non-optically smooth surfaces as it creates a speckle pattern, which breaks up the ideal Gaussian beam profile of the laser, in some cases making sub-pixel accuracy impossible and hence raising the uncertainty of the measurement. It should be noted that the speckle pattern noticed when measuring optically rough surfaces can be partially mitigated by taking multiple scans in the same vicinity of the laser spot and averaging the

scans out to reduce the effect of random speckle. However, this will ultimately reduce the measurement speed of laser scanning even further. Conversely, in fringe projection, as long as the roughness provides uniform scattering, does not cause high levels of light absorption, is consistent over the sample, and the reflected light is sufficiently higher than the noise on the camera CCD, the uncertainty of fringe projection is not affected as much by the object's roughness making it a more reliable technique for metal AM.

For post-process finished metal AM parts which are usually smooth enough not to disrupt the Gaussian profile of the incident laser beam, laser triangulation is more accurate than sinusoidal fringe projection as it can provide sub-pixel resolution, and is simpler as well, as the number and magnitude of uncertainty sources involved in the measurement are smaller which makes the calibration process easier. For maximum accuracy on smooth finished surfaces, therefore, laser scanning is recommended as the most favourable technique. The same conclusion is reached for parts with non-scattering light-absorbing surfaces because structured light systems have a lower optical power density and would not work as well as laser triangulation.

In terms of measurement latency one would expect the technique with the smallest inherent ambiguity to be faster at providing measurements. The ambiguity which exists in most fringe projection phase-shifting techniques due to the wrapped phase output being an inherent part of the measurement process is an issue that does not plague laser triangulation.¹⁰⁷ It is nevertheless possible to mitigate the presence of discontinuities through use of various unwrapping techniques,^{55,57,108} which of course carry a post-processing time penalty. As far as the overall measurement latency is concerned, however, in general structured light provides a faster measurement compared to laser triangulation even with all the post-processing required, as it can capture a whole view at once rather than raster scan a single laser beam over the measured object point-by-point (or row-by-row when using a laser line scanner). Hence, structured light systems are more applicable for industrial applications, as mass manufacturing industries try to minimise part inspection time and would ideally want to be able to use metrology *in situ* with the AM manufacturing process. There have been attempts to use "hybrid" techniques to speed up laser triangulation via use of incoherent light (see, for example, Ref. 109), whereby a projector is used to project multiple parallel white stripes on the surface instead of a sinusoidal fringe pattern. This facilitates a faster version of the laser stripe scanner concept because multiple parallel projected lines are shifted in unison across the object covering the field of view in a shorter time than would otherwise be required in order to scan a single laser line across the same field of view. However, classical sinusoidal fringe projection still outperforms this "hybrid" method¹⁰⁹ in a comparative analysis in both overall speed and accuracy.⁴⁴

In summary, form measurement of metal AM parts can be achieved using either a point-by-point or line-by-line (laser triangulation) or an areal field-of-view technique (structured light system). Both laser triangulation and structured light systems operate best on optically "rough" surfaces such as those nominally produced from metal AM, as they mostly

collect diffusely reflected light from the sample. However, for laser triangulation systems care must be taken as increase of roughness of the surface also increases speckle noise and hence the uncertainty of the measurement for laser triangulation systems, hence there is a trade-off between the amount of roughness required to collect light at the detector via diffuse reflection and the precision required by the measurement. There are some solutions that can be used to average out speckle noise by reducing the temporal and spatial coherence of the laser beam, but because they require mechanical movement of the laser, the measured object, or the medium in which the beam propagates, they usually also reduce the acquisition rate of the system. Antithetically, highly reflective smooth surfaces, such as those found in finished AM products, usually impede a structured light system from being able to efficiently overlay the required projected pattern onto the object, and thus either saturate the detector or reduce the SNR of the detected pattern dramatically. The light reflected from smooth surfaces is less of a problem for systems using laser triangulation due to their ability to work in "specular mode," but laser triangulation systems are also not immune to detector saturation from smooth reflective surfaces. If one technique were to be selected, therefore, sinusoidal fringe projection seems to be the more favourable option as it operates in a regime where both measurement speed and accuracy are better suited for industrial AM form metrology. Additionally, the uncertainty of the measurement is not affected as much by the surface roughness (as long as it is homogeneous over the part and does not cause extreme light absorption). It is suggested that laser triangulation would be useful as an alternative to fringe projection for measuring metal AM parts when higher noise rejection and measurement accuracy levels are required on smooth surfaces (i.e., when structured light methods fail to deliver), but the time penalty of these systems has to be taken into account. Measurement cycles in laser triangulation increase linearly as a function of the resolution required and hence laser triangulation might become prohibitively slow when measuring large parts. It is suggested that structured light systems be used to measure as-printed AM products and that laser triangulation be used for post-machined smooth metal AM products. In some cases, AM products are only partially machined; in which case, a combination of the two types of systems could be required to perform accurate measurements. It is noted that neither of these techniques can fully deal with deep occlusions or hidden structures present in metal AM systems as they rely on illumination and detection from a single angle and point of view and either new solutions or a fusion of data with an X-ray computed tomography system would be required for this to be overcome. The two solutions presented here, however, are able to measure the external form of metal AM parts which comes in use when these parts need to interface with other components in an assembly.

Looking into the future, the next generation of form measurement systems for metal AM, as mentioned in Section IV, could come from three sources. Presented in order of most likelihood these are, firstly the improvement of the software and hardware of current laser triangulation and structured light systems, secondly the use of promising techniques which have shown to have the necessary accuracy for industrial require-

ments but still have not been proved in the field and lastly from the development of high precision non-contact optical techniques to operate in non-laboratory conditions and with larger measurement ranges and fields of view.

Concerning the improvement of the software or hardware for laser triangulation and structured light systems, the obvious improvement could come from technology breakthroughs in imaging sensors with higher resolution, dynamic range, and the improvement of processing capabilities of both on-board and post-processing data. In terms of the use of new measurement methods demonstrated to have the appropriate accuracy, the most promising methods seem to be close range photogrammetry, Moiré profilometry, and active shape from focus as they have the smallest leap to perform in order to be applicable in industrial settings and can be more easily scaled up to larger fields of view. The other techniques depicted have a more rigid setup that is not easily scalable to larger fields of view and working distances. Lastly, the high-precision techniques discussed in Section V require much more development to be applicable for large fields of view and working distances, which means that they will be very expensive and complicated to apply in industrial settings and it is not foreseen that they will ever be used for post-process form measurement in metal AM.

ACKNOWLEDGMENTS

We would like to thank EPSRC Grant No. EP/M008983/1 for supporting this project and Dr. Simon Lawes (University of Nottingham) for reviewing the drafts.

- ¹Foresight Report, The Future of Manufacturing: A New Era of Opportunity and Challenge for the UK, 2013.
- ²W. Associates, *Additive Manufacturing Technology Roadmap for Australia Additive* (Wohlers Associates, Inc., 2011).
- ³S. L. N. Ford, "Additive Manufacturing Technology: Potential Implications for U.S. Manufacturing Competitiveness," *J. Int. Commer. Econ.* (published online September 2014).
- ⁴Additive Manufacturing in FP7 and Horizon 2020, 2014.
- ⁵P. Woolliams, J. Halstead, A. Morris, and R. Leach, in *NPL Additive Manufacturing Strategy* (2014).
- ⁶Measurement Science Roadmap for Metal-Based Additive Manufacturing, 2013.
- ⁷R. Quarshie, S. MacLachlan, P. Reeves, D. Whittaker, and R. Blake, *Shaping Our National Competency in Additive Manufacturing* (Technology Strategy Board, 2012).
- ⁸A. Allison and R. Scudamore, *Additive Manufacturing: Strategic Research Agenda* (2014).
- ⁹T. Wohlers and T. Caffrey, *Wohlers Report 2014*, available online at <https://www.wohlersassociates.com/2014report.htm>.
- ¹⁰S. Moylan, J. Slotwinski, A. Cooke, K. Jurrrens, and M. A. Donmez, *Lessons Learned in Establishing the NIST Metal Additive Manufacturing Laboratory* (National Institute of Standards and Technology, 2013).
- ¹¹E. G. Merriam, J. E. Jones, and L. L. Howell, in *Proceedings 42nd Aerospace Mechanisms Symposium NASA Goddard Sp. Flight Center*, 14–16 May 2014.
- ¹²I. A. Roberts, Ph.D. thesis, University of Wolverhampton, 2012.
- ¹³R. Paul, Ph.D. thesis, University of Cincinnati, 2013.
- ¹⁴E. Todorov, R. Spencer, S. Gleeson, M. Jamshidinia, and S. M. Kelly, *Non-destructive Evaluation (NDE) of Complex Metallic Additive Manufactured (AM) Structures*, 2014.
- ¹⁵A. Triantaphyllou, C. L. Giusca, G. D. Macaulay, F. Roerig, M. Hoebel, R. K. Leach, B. Tomita, and K. A. Milne, *Surf. Topogr. Metrol. Prop.* **3**, 024002 (2015).
- ¹⁶E. Savio, L. De Chiffre, and R. Schmitt, *CIRP Ann.—Manuf. Technol.* **56**, 810–835 (2007).
- ¹⁷*Coordinate Measuring Machines and Systems*, 2nd ed., edited by R. Hocken and P. Pereira (CRC Press, 2011).
- ¹⁸P. C. Hammett, L. G. Guzman, K. D. Frescolin, and S. J. Ellison, "Changing Automotive Body Measurement System Paradigms with 3D Non-Contact Measurement Systems," *SAE 2005 World Congress & Exhibition*, 2005.
- ¹⁹S. Rusinkiewicz, O. Hall-Holt, and M. Levoy, *ACM Trans. Graphics* **21**, 438 (2002).
- ²⁰O. Hall-Holt and S. Rusinkiewicz, *Proc. Eighth IEEE Int. Conf. Comput. Vision. ICCV 2001*, Vol. 2.
- ²¹F. Ullah, G. S. Lee, and K. Park, *Int. Conf. Inf. Sci. Appl.* **2**, 1 (2012).
- ²²Z. Wang, H. Du, and J. Barnes, *Exp. Mech.* **2**, 821 (2008).
- ²³S. S. Gorthi and P. Rastogi, *Opt. Lasers Eng.* **48**, 133 (2010).
- ²⁴N. Karpinsky and S. Zhang, *J. Real-Time Image Process.* **7**, 55 (2012).
- ²⁵S. Se and N. Pears, in *3D Imaging, Analysis and Applications* (Springer, 2012), Chap. 3, p. 95.
- ²⁶G. Sansoni, M. Trebeschi, and F. Docchio, *Sensors* **9**, 568 (2009).
- ²⁷S. Seitz, *An Overview of Passive Vision Techniques* (1999).
- ²⁸L. Smith, A10694 Development & Validation Process for 3D Point Cloud Gathering System, 2015.
- ²⁹D. Ahn, H. Kim, and S. Lee, *J. Mater. Process. Technol.* **209**, 664 (2009).
- ³⁰C. J. Luis Pérez, J. Vivancos Calvet, and M. A. Sebastián Pérez, *J. Mater. Process. Technol.* **119**, 52 (2001).
- ³¹R. Windecker, S. Franz, and H. J. Tiziani, *Appl. Opt.* **38**, 2837 (1999).
- ³²D. D. Gu, W. Meiners, K. Wissenbach, and R. Poprawe, *Int. Mater. Rev.* **57**, 133 (2012).
- ³³R. O. Ritchie, *Int. J. Fract.* **100**, 55 (1999).
- ³⁴J. Wang, R. K. Leach, and X. Jiang, *Surf. Topogr. Metrol. Prop.* **3**, 23001 (2015).
- ³⁵E. Herderick, in *Materials Science and Technology Conference and Exhibition 2011* (ASM International, 2011), pp. 1413–1425.
- ³⁶W. E. Frazier, *J. Mater. Eng. Perform.* **23**, 1917 (2014).
- ³⁷R. Leach, *Optical Measurement of Surface Topography* (Springer, 2011).
- ³⁸U. Schulz and K. Böhnke, *Commun. Comput. Inf. Sci.* **82**, 131–143 (2010).
- ³⁹H. Y. Feng, Y. Liu, and F. Xi, *Precis. Eng.* **25**, 185 (2001).
- ⁴⁰J. Zhang, J. Sun, Z. Liu, and G. Zhang, *Meas. Sci. Technol.* **25**, 105103 (2014).
- ⁴¹S. Zhang and S. Kiyono, *Measurement* **29**, 11 (2001).
- ⁴²P. Pavliček and G. Häusler, *Int. J. Optomechatronics* **8**, 292 (2014).
- ⁴³R. G. Dorsch, G. Häusler, and J. M. Herrmann, *Appl. Opt.* **33**, 1306 (1994).
- ⁴⁴J. Salvi, S. Fernandez, T. Pribanic, and X. Llado, *Pattern Recognit.* **43**, 2666 (2010).
- ⁴⁵J. Salvi, J. Pagès, and J. Battle, *Pattern Recognit.* **37**, 827 (2004).
- ⁴⁶P. S. Huang, S. Zhang, and F.-P. Chiang, *Opt. Eng.* **44**, 123601 (2005).
- ⁴⁷B. Carrhill and R. Hummel, *Comput. Vision, Graph. Image Process.* **32**, 337 (1985).
- ⁴⁸Y. Wang, Ph.D. thesis, Iowa State University, 2013.
- ⁴⁹Z. H. Zhang, *Opt. Lasers Eng.* **50**, 1097 (2012).
- ⁵⁰M. Takeda and K. Mutoh, *Appl. Opt.* **22**, 3977 (1983).
- ⁵¹Q. Kemao, *Appl. Opt.* **43**, 3472 (2004).
- ⁵²L. R. Watkins, *Opt. Lasers Eng.* **45**, 298 (2007).
- ⁵³L. R. Watkins, *Opt. Lasers Eng.* **50**, 1015 (2012).
- ⁵⁴S. Cui, D. Li, and Q. Li, *Opt. Lasers Eng.* **50**, 268 (2012).
- ⁵⁵R. Talebi and J. Johnson, in *17th International Conference on Image Processing, Computer Vision, and Pattern Recognition* (2013).
- ⁵⁶S. Zhang, in *Proceedings of SPIE*, edited by P. S. Huang, T. Yoshizawa, and K. G. Harding (SPIE Press, 2009), pp. 74320N-1–74320N-11.
- ⁵⁷M. J. Baker, Ph.D. thesis, University of Wollongong, 2008.
- ⁵⁸Z. Zhang, *IEEE Trans. Pattern Anal. Mach. Intell.* **22**, 1330 (2002).
- ⁵⁹M. Vo, Z. Wang, B. Pan, and T. Pan, *Opt. Express* **20**, 16926 (2012).
- ⁶⁰F. Sadlo, T. Weyrich, R. Peikert, and M. Gross, in *Processing Eurographics/IEEE VGTC Symp. Point-Based Graph* (2005).
- ⁶¹M. Kimura, M. Mochimaru, and T. Kanade, in *Processing IEEE Computer Society Conference on Computer Vision and Pattern Recognition* (2007).
- ⁶²J. Liao and L. Cai, in *IEEE/ASME International Conference on Advanced Intelligent Mechatronic (AIM)*, 2008, pp. 770–774.
- ⁶³H. Anwar, I. Din, and K. Park, *Int. J. Precis. Eng. Manuf.* **13**, 125 (2012).
- ⁶⁴J. Draréni, S. Roy, and P. Sturm, in *2009 IEEE Conference on Computer Vision and Pattern Recognition (IEEE, 2009)*, pp. 39–46.
- ⁶⁵J. Draréni, S. Roy, and P. Sturm, *Mach. Vision Appl.* **23**, 79 (2012).
- ⁶⁶S. Audet and M. Okutomi, in *2009 IEEE Conference on Computer Vision and Pattern Recognition, CVPR 2009 (IEEE, 2009)*, pp. 47–54.
- ⁶⁷I. Martynov, J. K. Kamarainen, and L. Lensu, *Image Anal.* **6688**, 536–544 (2011).

- ⁶⁸X. Chen, J. Xi, Y. Jin, and J. Sun, *Opt. Lasers Eng.* **47**, 310 (2009).
- ⁶⁹P. S. Huang, *Opt. Eng.* **45**, 083601 (2006).
- ⁷⁰D. Moreno and G. Taubin, in *Proceedings of 2nd Joint. 3DIM/3DPVT Conference 3D Imaging, Modeling Processing Visualization and Transmission 3DIMPVT 2012* (IEEE, 2012), pp. 464–471.
- ⁷¹J. Geng, *Adv. Opt. Photonics* **3**, 128 (2011).
- ⁷²H. Guo, H. He, and M. Chen, *Appl. Opt.* **43**, 2906 (2004).
- ⁷³S. Ma, C. Quan, R. Zhu, L. Chen, B. Li, and C. J. Tay, *Opt. Commun.* **285**, 533 (2012).
- ⁷⁴S. Zhang and S. Yau, *Appl. Opt.* **46**, 36 (2007).
- ⁷⁵B. Pan, Q. Kema, L. Huang, and A. Asundi, *Opt. Lett.* **34**, 416 (2009).
- ⁷⁶Y. R. Huddart, Ph.D. thesis, Heriot-Watt University, 2010.
- ⁷⁷G. Häusler, J. H. Less, M. Maul, and H. Weissmann, *Appl. Opt.* **27**, 4638 (1988).
- ⁷⁸S. K. Nayar, M. Watanabe, and M. Noguchi, *IEEE Trans. Pattern Anal. Mach. Intell.* **18**, 1186 (1996).
- ⁷⁹D. M. Meadows, W. O. Johnson, and J. B. Allen, *Appl. Opt.* **9**, 942 (1970).
- ⁸⁰H. Takasaki, *Appl. Opt.* **9**, 1467 (1970).
- ⁸¹J. A. N. Buytaert and J. J. J. Dirckx, *J. Opt. Soc. Am. A* **24**, 2003 (2007).
- ⁸²J. A. N. Buytaert and J. J. J. Dirckx, *Opt. Express* **16**, 179 (2008).
- ⁸³A. K. Asundi, S. R. Marokkey, G. G. Olson, and J. N. Walker, *Proc. SPIE* **2347**, 270–275 (1994).
- ⁸⁴G. E. Sommargren, *Appl. Opt.* **20**, 610 (1981).
- ⁸⁵B. P. Hildebrand and K. A. Haines, *J. Opt. Soc. Am.* **57**, 155 (1967).
- ⁸⁶C. Quan, H. M. Shang, C. J. Tay, and P. J. Bryanston-Cross, *Opt. Lasers Eng.* **30**, 351 (1998).
- ⁸⁷J. W. Wagner, in *Review of Progress in Quantitative Nondestructive Evaluation*, edited by D. O. Thompson *et al.* (Plenum Press, New York, 1988), pp. 1177–1184.
- ⁸⁸J. E. Millerd and N. J. Brock, *Appl. Opt.* **36**, 2427 (1997).
- ⁸⁹M. Yokota and T. Adachi, *Appl. Opt.* **50**, 3937 (2011).
- ⁹⁰G. Pedrini, P. Fröning, H. J. Tiziani, and M. E. Gusev, *Appl. Opt.* **38**, 3460 (1999).
- ⁹¹A. A. Friesem and U. Levy, *Appl. Opt.* **15**, 3009 (1976).
- ⁹²P. J. Van Heerden, *Appl. Opt.* **2**, 393 (1963).
- ⁹³A. Sinha, W. Sun, T. Shih, and G. Barbastathis, *Appl. Opt.* **43**, 1533 (2004).
- ⁹⁴W. Liu, D. Psaltis, and G. Barbastathis, *Opt. Lett.* **27**, 854 (2002).
- ⁹⁵W. Sun, *Profilometry with Volume Holographic Imaging* (Massachusetts Institute of Technology, 2006).
- ⁹⁶F. Aflatouni, B. Abiri, A. Rekhi, and A. Hajimiri, *Opt. Express* **23**, 5117 (2015).
- ⁹⁷E. P. Baltasvias, *ISPRS J. Photogramm. Remote Sens.* **54**, 83 (1999).
- ⁹⁸Z. Wang, R. Liu, T. Sparks, H. Liu, and F. Liou, *Precis. Eng.* **42**, 1 (2015).
- ⁹⁹R. J. Woodham, *Opt. Eng.* **19**, 139 (1980).
- ¹⁰⁰L. M. Galantucci, G. Percoco, and R. Ferrandes, *Rev. Int. Ing. Numer.* **2**, 29 (2006).
- ¹⁰¹L. M. Galantucci, F. Lavecchia, and G. Percoco, *J. Comput. Inf. Sci. Eng.* **13**, 044501 (2013).
- ¹⁰²W. Zhaoyang, D. Fulong, and J. Xiaolin, *Acta Mech. Sin.* **15**, 176 (1999).
- ¹⁰³P. J. Caber, *Appl. Opt.* **32**, 3438 (1993).
- ¹⁰⁴H. Muhamedsalih, Ph.D. thesis, University of Huddersfield, 2013.
- ¹⁰⁵T. Widjanarko, Ph.D. thesis, Loughborough University, 2011.
- ¹⁰⁶R. Danzl, F. Helml, and S. Scherer, *Strojniški Vestn.–J. Mech. Eng.* **2011**, 245 (2011).
- ¹⁰⁷S. Zhang, *Opt. Lasers Eng.* **48**, 149 (2010).
- ¹⁰⁸Z. Huang, A. J. Shih, and J. Ni, *Meas. Sci. Technol.* **17**, 3110 (2006).
- ¹⁰⁹J. Guehring, in *Proceedings of SPIE, Videometrics Optical Methods for 3D Shape Measurement*, edited by S. F. El-Hakim and A. Gruen (SPIE Press, 2000), Vol. 4309, pp. 220–231.